7-2015

Nonstationarity in seasonality of extreme precipitation: A nonparametric circular statistical approach and its application.

Nirajan Dhakal
University of Maine

Shaleen Jain
University of Maine

Alexander Gray
University of Maine

Michael Dandy

Esperanza Stancioff

AGU PUBLICATIONS

Water Resources Research

RESEARCH ARTICLE
10.1002/2014WR016399

Nonstationarity in seasonality of extreme precipitation: A nonparametric circular statistical approach and its application

Nirajan Dhakal[1,2,3], Shaleen Jain[1,2,4], Alexander Gray[1,5], Michael Dandy[2], and Esperanza Stancioff[1,5]

[1]Senator George J. Mitchell Center for Sustainability Solutions, University of Maine, Orono, Maine, USA, [2]Department of Civil and Environmental Engineering, University of Maine, Orono, Maine, USA, [3]Northeast Climate Science Center, Amherst, Massachusetts, USA, [4]Climate Change Institute, University of Maine, Orono, Maine, USA, [5]Sea Grant Program, University of Maine Cooperative Extension, Waldoboro, Maine, USA

Key Points:
- Distribution of extreme precipitation dates often exhibits multiple modes
- Nonparametric circular statistical approach characterizes changes in seasonality
- New method allows for an adaptive estimation of seasonal probability density

Supporting Information:
- Supporting Information S1

Correspondence to:
N. Dhakal,
ndhakal@umass.edu

Citation:
Dhakal, N., S. Jain, A. Gray, M. Dandy, and E. Stancioff (2015), Nonstationarity in seasonality of extreme precipitation: A nonparametric circular statistical approach and its application, *Water Resour. Res.*, *51*, 4499–4515, doi:10.1002/2014WR016399.

Received 14 SEP 2014
Accepted 22 MAY 2015
Accepted article online 30 MAY 2015
Published online 21 JUN 2015

Abstract Changes in seasonality of extreme storms have important implications for public safety, storm water infrastructure, and, in general, adaptation strategies in a changing climate. While past research on this topic offers some approaches to characterize seasonality, the methods are somewhat limited in their ability to discern the diversity of distributional types for extreme precipitation dates. Herein, we present a comprehensive approach for assessment of temporal changes in the calendar dates for extreme precipitation within a circular statistics framework which entails: (a) three measures to summarize circular random variables (traditional approach), (b) four nonparametric statistical tests, and (c) a new nonparametric circular density method to provide a robust assessment of the nature of probability distribution and changes. Two 30 year blocks (1951–1980 and 1981–2010) of annual maximum daily precipitation from 10 stations across the state of Maine were used for our analysis. Assessment of seasonality based on nonparametric approach indicated nonstationarity; some stations exhibited shifts in significant mode toward Spring season for the recent time period while some other stations exhibited multimodal seasonal pattern for both the time periods. Nonparametric circular density method, used in this study, allows for an adaptive estimation of seasonal density. Despite the limitation of being sensitive to the smoothing parameter, this method can accurately characterize one or more modes of seasonal peaks, as well as pave the way toward assessment of changes in seasonality over time.

1. Introduction

The conventional approach to interpreting Earth's climatic variability—based on variables such as precipitation and temperature—assumes that event recurrence and their distribution can be understood as largely time-invariant statistical processes (often termed as the stationarity assumption). As a result, numerous societal concerns, such as public safety and infrastructure design benefit from place-based estimates of rare event statistics, such as the magnitude of 100 year rain event etc. In the United States, NOAA Rainfall Frequency Atlas is an important resource for this information [*Hershfield*, 1961]. Such statistical characterization of historical weather and climatic risk allows decision makers to choose levels of protection against extreme weather events; however, an underlying assumption is that the past is a good analog for the future. The assumption of hydroclimatic stationarity is being increasingly questioned, and has led to stimulating discussions in environmental science literature [e.g., *Jain and Lall*, 2000, 2001; *Milly et al.*, 2008; *Montanari and Koutsoyiannis*, 2014]. Departures from the stationary statistics of weather and climate variables stem from periodicities and trends, as well as changes within the earth system (such as transformation of pristine landscapes stemming from urbanization).

While there is a significant and growing body of knowledge (case studies and methodologies) related to changes in the magnitude of extreme precipitation [*Karl and Knight*, 1998; *Groisman et al.*, 2001; *DeGaetano*, 2009; *Higgins and Kousky*, 2013], little attention has been devoted to changes in their seasonality (for example, based on the calendar date of extreme events). Significant changes in seasonality of extreme events not only challenge infrastructure and asset management, potentially the increased complexity of events and impacts also require distinct responses. For example, in the case of culverts, a pervasive element of stormwater infrastructure, extreme rain events during different seasons result in a diversity of flooding conditions. For example, in cold regions, malfunctioning culverts in Winter and Spring suffer from blockages due to ice; Summer and Fall season rain events result in debris and brush buildup, thus reducing flow volumes conveyed. Thus, an understanding of shifts toward new extreme event seasons or weakening and intensification within known

seasonal windows has significance for characterization of local hydroclimatic change, as well as usable knowledge to inform adaptation efforts. In this study, we consider the following research question: *What are some robust approaches to understand and characterize the nature and extent of changes in seasonality of extreme precipitation?* To this end, we present a fresh empirical statistical approach and case study from New England region. In answering this question, this work complements the emerging research literature that focuses on nonstationarity from the standpoint of extreme event magnitude and intensity [*Khaliq et al*., 2006; *Mirhosseini et al*., 2013; *Salas and Obeysekera*, 2013; *Cheng and AghaKouchak*, 2014].

In the past, several methods have been used to analyze trends in seasonality of precipitation characteristics. Some of these methods are based on estimation of seasonality index from mean monthly rainfall and mean annual rainfall [*Walsh and Lawler*, 1981]. Other methods are based on estimation of linear trends in precipitation extremes for four traditionally fixed meteorological seasons: Winter - starting December 1 and ending February 28 (February 29 in a Leap Year)(DJF), Spring - starting March 1 and ending May 31 (MAM), Summer - starting June 1 and ending August 31 (JJA), and Fall (Autumn) - starting September 1 and ending November 30 (SON) [*Moberg et al*., 2006; *Zolina et al*., 2008]. Relatively few studies have examined the change in the timing or seasonality [*Pal et al*., 2013]. *Rajagopalan and Lall* [1995] examined the change in seasonality of daily precipitation in the western United States using a nonparametric approach based on nonhomogeneous Poisson process applied to precipitation records before and after 1950. *Pryor and Schoof* [2008] investigated the seasonality of precipitation over contiguous U.S. by analyzing change in the calendar date on which a certain percentile of annual total precipitation was achieved for three different 30 year time periods between 1911 and 2000. More recently, *Pal et al*. [2013] documented station-specific shifts in wet and dry seasons over U.S. based on Markovian precipitation models. While the published literature offers useful methods to characterize seasonality, these approaches are somewhat limited in their ability to discern the diversity of distributional types for extreme precipitation dates. Seasonal weather and atmospheric moisture pathways show regional patterns, often determined by the large-scale, general circulation of the atmosphere [*Hirschboeck*, 1988]. These factors can greatly influence the length and number of seasonal precipitation windows within a year. As a result, the probability distribution of extreme event timing tends to be more often multimodal and less well aligned with calendar months and predefined seasons.

Given the limitations noted above, we developed a robust statistical approach for seasonality assessment based on directional/circular statistics [*Mardia and Jupp*, 2000; *Jammalamadaka and SenGupta*, 2001] applied to hydroclimatic variables. Directional/circular statistics is a branch of statistics that deals with directions, where random variables are represented by angles measured with respect to some starting point and sense of rotation [*Jammalamadaka and SenGupta*, 2001]. Standard statistical methods used for analysis of ordinary linear data (for example, like computing the sample mean and the sample variance) are inappropriate for analysis of circular data [*Mardia and Jupp*, 2000; *Jammalamadaka and SenGupta*, 2001; *Lee*, 2010]. Judicious use of circular statistics provides an improved understanding of environmental variables modeled as circular random processes (for example, the timing of an event within a cycle). In this study, daily precipitation records were used to derive time series of calendar dates for annual maximum daily precipitation, and analyzed using circular parametric and nonparametric statistical approaches. Circular probability distributions assign probabilities to each point on the circumference of a unit circle representing a direction (discussed in detail later). Although the issue of seasonality characterization for precipitation has been recognized for over a century [*Cook*, 1910], to our knowledge, very few studies have used the circular approach for seasonality assessment of extreme rainfall or other hydrologic variables. *Markham* [1970] made an initial attempt by representing mean monthly rainfall totals as vectors whose magnitude and direction were denoted, respectively, by the mean monthly values and their time of occurrence over the calendar year. Later *Bayliss and Jones* [1993] and *Burn* [1997] used the circular approach for seasonality assessment of hydrological extreme events by considering the mean date and variability of occurrence of extreme events. *Parajka et al*. [2009, 2010] used a similar approach to evaluate seasonality of precipitation and streamflow records. More recently, *Lee et al*. [2012] used circular statistical approach to determine regionalization of extreme precipitation across South Korea. All the previous studies based on circular statistical approaches employ two summary statistical measures to characterize seasonality. The inability of these traditional summary statistics to detect and model event-timing distributions with multiple seasons remains a significant challenge. Nonparametric circular density approach, presented in this study, offers an adaptive and robust alternative. To this end, such an approach can accurately characterize one or more modes representing seasonal peaks, as well as pave the way for an assessment of changes in seasonality over time. Results have salience for both hydroclimatic change studies and infrastructure adaptation

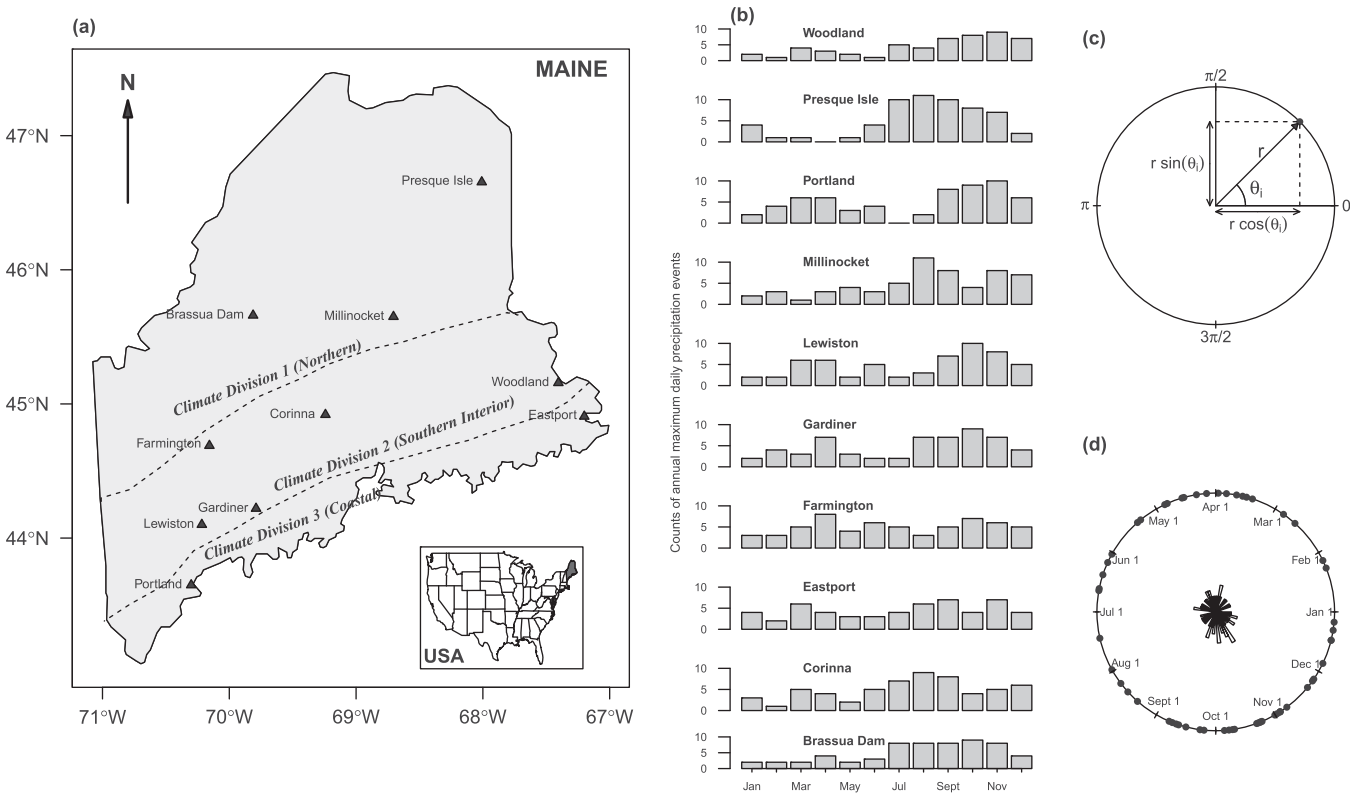

Figure 1. (a) A map of the study region, climate divisions, and locations of 10 long-term U.S. Historical Climatology Network precipitation stations in Maine, (b) histograms showing counts of annual maximum daily precipitation per each month of the year for the period 1951–2010 ($n = 60$), (c) circular plot showing the date of occurrence of a particular event within a year on the circumference of a unit circle centered at origin, and (d) circular plot of annual maximum daily precipitation for the period 1951–2010 for Lewiston, Maine. A Rose diagram (which is equivalent to the histogram for the linear case) is also shown to represent frequencies of annual maximum daily precipitation event dates.

considerations. It is worth noting that this work augments the rich body of knowledge in statistical hydrology, wherein nonparametric approaches have been used profitably in flood estimation, streamflow, and rainfall modeling [e.g., *Lall*, 1995]. However, this is the first study to use circular statistical approach within a nonparametric framework for hydrologic application.

1.1. Data and Study Region

The state of Maine, located in the northeastern region of the United States, is divided into three climate divisions by National Weather Service: Northern, Southern Interior, and Coastal (Figure 1a). These climate divisions cover 54%, 31%, and 15% of the state's total area, respectively [*Jacobson et al.*, 2009]. The elevation in Maine ranges from 0 to 1606 m above sea level. The average annual precipitation (in three climate divisions) ranges between 1016 and 1168 mm (40 and 46 in.) [*Sen Gupta et al.*, 2011]. At the climate division level, no appreciable patterns in seasonality are seen, however, the coastal region is wettest in winter, while in the north, summer is slightly wetter than winter [*Jacobson et al.*, 2009].

For this study, daily precipitation records for the 1951–2010 period from 12 stations across the state of Maine were obtained from the Historical Climatology Network database [*Easterling et al.*, 1996]. A number of records in this database are incomplete. Following screening criteria were used for this study: (a) percentage of missing values per year less than 20%, and (b) record length greater than or equal to 50 years. Of the 12 precipitation records (Figure 1a), two (Houlton and Acadia National Park) were excluded; fewer than 50 years of records were available for analysis for both stations. For all the remaining 10 stations, each of the months consists of at least 93% of the data set (Figure S1).

1.2. Seasonality Characterization of Extreme Precipitation

A preliminary assessment of seasonality is based on an examination of total counts of annual maximum daily precipitation events that fall on each month of the year over the 60 year historical record. Histograms

depicting these counts are shown in Figure 1b. We also estimated the percentage of such counts for four fixed seasons: Winter (DJF), Spring (MAM), Summer (JJA), and Fall (SON), and listed in Table S1. From Figure 1b and Table S1, we can see that both monthly and seasonal counts exhibit remarkable diversity across 10 stations. For example, for stations like Presque Isle and Brassua Dam, majority of extreme precipitation events occur during Summer (JJA) and Fall (SON) seasons (Table S1). While for stations like Portland and Lewiston, in addition to the Summer and Fall seasons, there is significant portion of events occurring during Winter (DJF) and Spring (MAM) seasons. On the other hand, counts for stations like Farmington and Eastport show more or less uniform behavior with extreme precipitations occurring evenly throughout all the four seasons. Such complex behavior observed in seasonal distribution of extreme event counts affirms the need for a superior technique for more clear and accurate representation of seasonality.

As noted above, a robust approach to characterize seasonality is by using the circular statistical approach. A circular statistical approach considers the date of occurrence of particular event within a year as polar coordinates on the circumference of a unit circle centered at origin as shown in Figure 1c [*Jammalamadaka and SenGupta*, 2001]. Note that for Figure 1c, r = 1 and each direction (θ_i) thus corresponds to a point on the circumference of the unit circle. The angular position of the date of occurrence (D) of an extreme precipitation event "i" is defined using:

$$\theta_i = D_i\left(\frac{2\pi}{365}\right) \tag{1}$$

where θ_i is the angular value (in radians) for the extreme event "i," $D = 1$ for 1 January and $D = 365$ for 31 December ($D = 366$ for leap year); analogously, in terms of angular value in radians, 0 radian corresponds to 1 January and 2π radian corresponds to 31 December. For a sample of n extreme precipitation events, this information can be plotted on a circle to provide a visual representation of seasonality. Figure 1d shows such a graphical representation of annual maximum daily precipitation for the period 1951–2010 for Lewiston, Maine. A Rose diagram (which is equivalent to the histogram for the linear case) for this data set is also shown.

From a sample of n extreme precipitation events, the x and y coordinates of the mean extreme precipitation date around the year are determined using:

$$\bar{x} = \frac{\sum_{i=1}^{n} \cos(\theta_i)}{n} \tag{2}$$

$$\bar{y} = \frac{\sum_{i=1}^{n} \sin(\theta_i)}{n} \tag{3}$$

where $\bar{x}$ and $\bar{y}$ are the x and y coordinates of the mean extreme precipitation date. The direction representing mean date of occurrence of n extreme precipitation events is then obtained using:

$$\bar{\theta} = \tan^{-1}\left(\frac{\bar{y}}{\bar{x}}\right) \tag{4}$$

The variability of n extreme precipitation event occurrences about the mean date is obtained using the mean resultant length:

$$\rho = \frac{\sqrt{\bar{x}^2 + \bar{y}^2}}{n} \tag{5}$$

ρ is a dimensionless measure of the spread of the data and the value of ρ ranges from 0 (indicating greater variability in the date of occurrence of extreme precipitation events) to 1 (indicating all the extreme precipitation events occurred on the same day of the year). Four previous studies [*Bayliss and Jones*, 1993; *Burn*, 1997; *Parajka et al*., 2009, 2010] have used angular representation of seasonality (similar to equations (1)–(5)) for analysis of precipitation and streamflow records.

The circular standard deviation (*csd*) is calculated based on the following equation [*Mardia and Jupp*, 2000]:

$$csd = \sqrt{-2\ln\rho} \tag{6}$$

Parameters $\overline{\theta}$, ρ, and *csd* offer simplified and accessible station-by-station summary of annual maximum daily precipitation variability for the 1951–2010 period (Table 1). Values of $\overline{\theta}$ range from 2.91 to 5.60,

Table 1. Seasonality of Annual Maximum Daily Precipitation for 1951–2010 Period, Estimated From the Circular Statistical Analysis

	Circular Statistics			
	Mean		Variability	Standard
Station	$(\bar{\theta})^a$	Day of Year	$(\rho)^b$	Deviation $(csd)^c$
Brassua Dam	4.41	256 (11 Sep)	0.34	1.46
Corinna	4.12	240 (26 Aug)	0.25	1.66
Eastport	4.76	277 (2 Oct)	0.13	2.01
Farmington	2.91	169 (17 Jun)	0.04	2.59
Gardiner	4.79	278 (4 Oct)	0.19	1.83
Lewiston	5.08	295 (20 Oct)	0.17	1.90
Millinocket	4.55	265 (20 Sep)	0.31	1.53
Portland	5.60	325 (20 Nov)	0.20	1.79
Presque Isle	4.34	252 (8 Sep)	0.49	1.19
Woodland	4.93	287 (12 Oct)	0.35	1.44

[a]Equation (4).
[b]Equation (5).
[c]Equation (6).

indicating the computed means corresponding to 17 June and 20 November, respectively. Based on the calendar day corresponding to the estimated $\overline{\theta}$, we can see that a majority of estimates fall within the September–October. Values of ρ range from 0.04 to 0.49, and values of *csd* range from 1.19 to 2.29. Based on ρ and *csd*, we can see that for Presque Isle ($\rho = 0.49$, $csd = 1.19$), there is strong unimodal pattern; while for Farmington ($\rho = 0.04$, $csd = 2.59$) there is no seasonal pattern. Moreover, a number of stations like Portland ($\rho = 0.20$, $csd = 1.79$) and Lewiston ($\rho = 0.17$, $csd = 1.90$) exhibit bimodal pattern. It is interesting to note that for both stations in the Coastal climate division (Portland and Eastport) as well as three other nearby stations in the Southern Interior climate division (Lewiston, Woodland, and Gardiner), the mean date of occurrence $\overline{\theta}$ falls during October–November. On the other hand, variability is lower (indicated by higher values of ρ and lower values of *csd*) for all the three stations (Brassua Dam, Presque Isle, and Millinocket) in the Northern climate division.

Linear and circular statistical analysis of precipitation extremes (Figure 1b and Table 1) reinforces the view that there is significant diversity in the patterns of seasonality, when computed based on the distribution of event dates. In general, unimodal distributions appear more an exception than a rule in the analysis of daily precipitation extreme dates. Careful diagnosis of the nature of data is warranted for accurate assessment of seasonality.

1.3. Seasonality of Synthetic Data

To develop a clear appreciation of the relative merits of the three circular statistical measures (equations (4)–(6)), we generated three different types of synthetic data for analysis of seasonality using circular statistical measures. As noted in the case of historical records analyzed in the previous section, we anticipate that our three example cases broadly span the range of distribution types found in nature. Three different types of synthetic data, with a sample size of 30, with their frequency distribution are shown in Figure 2. Figure 2a represents "pseudo" uniform data with no preferred direction (uniform distribution discussed in detail later); Figure 2b represents "pseudo" unimodal data concentrated from January to April; Figure 2c represents "pseudo" trimodal data concentrated from October to December, February to April, and June to August.

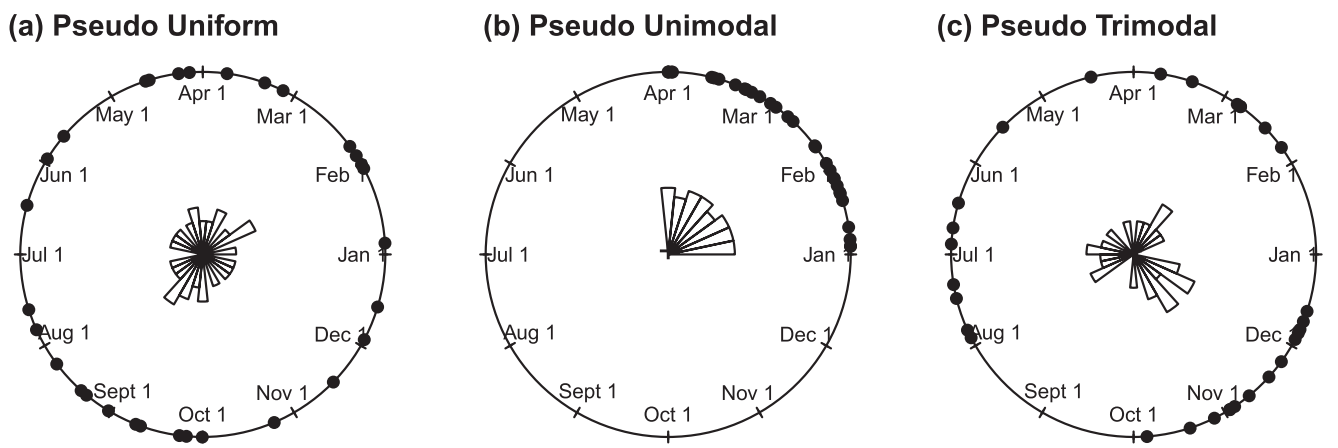

Figure 2. Three types of synthetic data ($n = 30$) plots and their Rose diagrams: (a) "pseudo" uniform data with no preferred direction, (b) "pseudo" unimodal data concentrated from January to April, and (c) "pseudo" trimodal data concentrated in the following seasonal windows: October–December, February–April, and June–August.

Table 2. Seasonality of Three Distinct Cases of the Synthetic Data, Estimated From the Circular Statistical Analysis

	Circular Statistics			Uniformity Tests			Hewitt Test
Synthetic Data Case	$\overline{\theta}$	ρ	*csd*	Rayleigh	Rao Spacing	Kuiper	Maximum Rank Sum (3 Month Window)
Uniform (a)	3.96 (17 Aug)	0.02	2.69	0.02	108.63	0.94	29
Unimodal (b)	0.80 (15 Feb)	0.89	0.49	0.89**	261.02**	4.30**	33**
Trimodal (c)	5.79 (1 Dec)	0.20	1.79	0.20	149.74	1.61	31

**p value $\leq$ 0.05; *0.05 $<$ p value $<$0.1.

The prefix "pseudo" is added to signify the limited sample size-based representation of the underlying distribution types.

Values of $\overline{\theta}$, ρ, and *csd* estimated for three cases of synthetic data are presented in Table 2. For "pseudo" uniform data (case (a)), as expected, ρ is small and *csd* is high indicating no seasonal peaks. For "pseudo" unimodal data (case (b)), as expected, ρ is high and *csd* is low indicating strong seasonality. For "pseudo" trimodal data (case (c)) ρ is small and *csd* is high; $\overline{\theta}$ for this case indicates that the mean date of occurrence is 1 December. However, this estimated circular mean is a misleading indicator of the dominant season. A small value of ρ (0.20) indicates that the extreme event date is highly variable; however, the nature of preferred seasonal windows or modes is not captured by this metric.

In addition to the estimation of three statistical parameters, $\overline{\theta}$, ρ, and *csd*, another approach to analyze and understand the nature of seasonal distribution uses well-designed statistical tests to assess the relative fit of the data set to a probability distribution type. In general, a system with preferred seasonality shows departures from uniformity/uniform distribution. Three nonparametric uniformity tests have been used and tested extensively in the circular statistics literature: Rayleigh Test, Rao Spacing Test, and Kuiper Test [*Mardia and Jupp*, 2000; *Jammalamadaka and SenGupta*, 2001]. For example, *Fahidy* [2013] applied these three tests to chemical process analysis. A null hypothesis of no seasonal preference in extreme precipitation event dates can be tested efficiently with these approaches. Rayleigh test is based on the significance of the mean resultant length ρ [*Jammalamadaka*, 1972; *Mardia and Jupp*, 2000]. The alternative hypothesis of this test is a unimodal distribution with unknown mean direction and unknown mean resultant length. Evidently, the hypothesis of uniformity is rejected when ρ is too large. Hence, this test is efficient for the seasonality assessment for those cases where there is strong unimodal seasonal pattern or no seasonal (uniform) pattern. Rao Spacing test is based on the sample arc length. For n observations, Rao Spacing test statistic can be interpreted as the uncovered part of the circumference when n arcs of length $1/n$ are placed starting with each of the n observed points on the circle [*Jammalamadaka and SenGupta*, 2001]. Hence, if the underlying distribution is uniform, n successive observations should be approximately evenly spaced. Note that the circular uniform distribution for our case represents "no seasonality." Wherefore, large deviations from this distribution resulting from unusually large spaces or unusually short spaces between observations are evidence for seasonality. According to *Fahidy* [2013], Rao Spacing test is more prone to reject the null hypothesis than the Rayleigh and the Kuiper test since it carries a smaller Type I error; however, based on the nature of the statistical data, rejection of null hypothesis cannot be absolutely certain. Kuiper test is based on the hypothesis that the observations come from a population with a specified empirical distribution function. Kuiper test statistic is a rotation-invariant Kolmogorov-type test statistic [*Jammalamadaka and SenGupta*, 2001]. It measures the distance between the cumulative uniform distribution function and the empirical distribution function.

Test statistics from all three tests are presented in Table 2 for each of synthetic data. As expected, for the "pseudo" uniform data (case (a)), the null hypothesis of uniformity is accepted indicating no seasonality, and for the "pseudo" unimodal data (case (b)), the null hypothesis of uniformity is rejected indicating seasonality. However, for the "pseudo" trimodal data (case (c)) also the null hypothesis of uniformity is accepted indicating no seasonality. It is worth noting from Table 2 that for all the three uniformity tests, larger values of the test statistic indicate proclivity toward clustering or seasonality. Also based on our analysis of different types of synthetic data (not shown here), we noticed that Rayleigh test is powerful (nonuniform) against unimodal but not against multimodal alternatives of uniformity. Both Rao Spacing and Kuiper tests are consistent (nonuniform) against unimodal as well as multimodal alternatives; Rao Spacing test being more powerful among these two tests. However, none of these tests can capture the actual nature of

seasonality for complex data as encountered in case (c). In other words, when any of these tests is not rejected, we cannot conclude that the data follow the uniform distribution or there is no seasonal pattern (as for case (c)). Rather, there is insufficient evidence to reject the null hypothesis of uniformity.

We also used a nonparametric test based on work of *Hewitt et al*. [1971] and *Rogerson* [1996] to test the null hypothesis of no seasonality against the alternative hypothesis of seasonality in the data. One interesting aspect of this approach is the ability to incorporate prior knowledge (for example, window lengths based on the climatological length of rainy season at the location) in analyses. *Hewitt et al*. [1971] developed seasonality test in the monthly data based on maximum rank-sum observed for any six-consecutive period. Later, *Rogerson* [1996] generalized this test, where the peak period can be 3, 4, or 5 months. In our case, we used peak period of 3 months to estimate Hewitt's test statistic, and the results are listed in Table 2. Results obtained are similar to those from the three uniformity tests used above; while uniform and unimodal cases are relatively well assessed by the statistical tests; the multimodal cases need a more comprehensive approach, perhaps with attention to local changes in the probability density. To sum up, methods based on three summary statistics, and four uniformity tests are useful for assessing seasonality for simple data like cases (a) (unimodal) and (b) (uniform), while for more complex data like case (c), results from one or all of these methods may be misleading. To this end, our nonparametric circular approach, which offers a locally adaptive methodology to analyze the diversity of distributions types, including multimodality is presented next.

2. Robust Characterization of Seasonality

Figure 3 provides a schematic representation of a circular analysis approach for the seasonality assessment, which includes comprehensive analysis of seasonality based on the statistical tests discussed in the previous section, as well as a new nonparametric density approach described below. Computations were performed on the R Statistical Computing Platform, and utilized the statistical package "circular" [*Agostinelli and Lund*, 2013]. For the nonparametric circular method, extreme precipitation dates were used to compute the circular probability distribution. Four previous studies [*Bayliss and Jones*, 1993; *Burn*, 1997; *Parajka et al*., 2009, 2010] have used the circular statistical approach for assessing the seasonality. However, no work to our knowledge has been devoted to the seasonality of extreme precipitation. Circular statistical approach assigns probabilities to each point on the circumference (of a unit circle) representing a direction. In other words, circular distribution is a way of defining directional distributions. In our case, each data point is the angular position of the occurrence date of extreme precipitation events and circular distribution represents the seasonal distribution of these dates. For circular distribution, the density estimates (and their properties) depend on the selection of the smoothing kernel (in our case, the von Mises distribution) and its smoothing parameter, known as bandwidth. The von Mises distribution or a Circular Normal distribution is a symmetric unimodal distribution with probability density function:

$$f(\theta;\mu,\kappa)=\frac{1}{2\pi I_0(\kappa)}e^{\kappa\cos(\theta-\mu)},\quad 0\le\theta<2\pi, \tag{7}$$

where $0\le\theta<2\pi$ is a mean direction, $\kappa\ge 0$ is a concentration parameter, and $I_0(\kappa)$ is the modified Bessel function of the first kind and order zero [*Jammalamadaka and SenGupta*, 2001, section. 2.2.4]. The von Mises probability distribution is symmetric about the directions μ and $\mu+\pi$ (by the symmetry of the *cosine* function). Since the *cosine* function has maximum value at $\theta=\mu$, the mean direction, μ, coincides with the modal direction. The parameter, κ, measures the concentration toward the mean direction μ in such a way that, as the value of κ increases, the higher will be the concentration toward the mean direction μ (Figure S2). In other words, the concentration parameter plays the role of the smoothing parameter (or bandwidth) for the circular probability density estimation using the von Mises kernel. As the overall density estimate is sensitive to the choice of bandwidth, a discussion of results obtained for our data is presented next. Readers are referred to *Mardia and Jupp* [2000] and *Jammalamadaka and SenGupta* [2001] for additional details regarding circular distributions and their properties.

2.1. Bandwidth Selection

Numerous approaches have been developed for bandwidth selection in circular density estimation. For example, data-driven procedures were proposed by *Hall et al*. [1987] using cross-validation method.

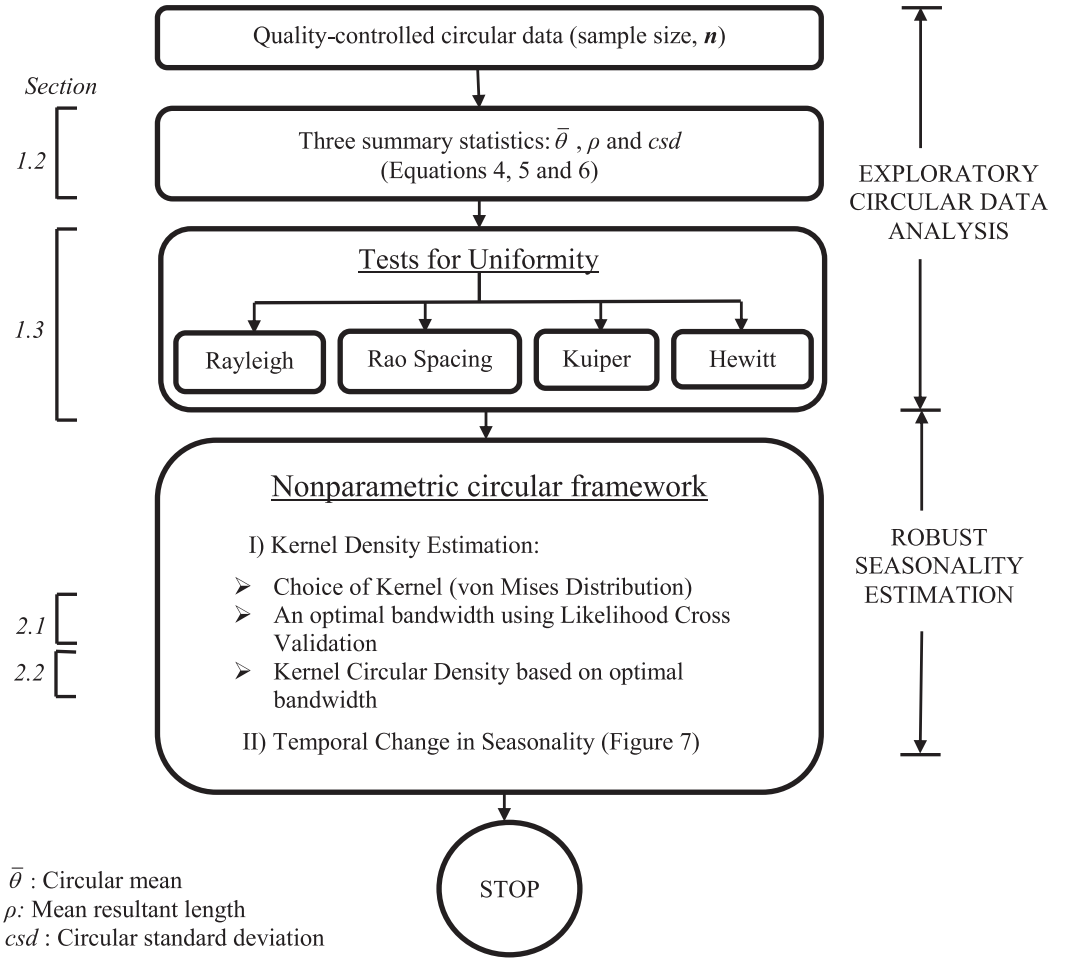

Figure 3. Schematic diagram showing a comprehensive circular analysis approach for the seasonality assessment; three summary statistics, four statistical tests, and a nonparametric approach are pursued to provide a robust assessment of the nature of probability distribution and changes therein.

Taylor [2008] derived a rule of thumb that consists of minimizing the asymptotic mean integrated squared error. More recently, *Oliveira et al*. [2012] introduced a plug-in procedure for bandwidth selection in kernel circular density estimation. For any of these methods, the chosen bandwidth minimizes some error criterion. Bandwidth for our study was estimated using the likelihood cross-validation method (*LCV*). *LCV* method selects a bandwidth that maximizes the likelihood cross-validation function [*Oliveira et al*., 2013, equation (8)]. *LCV* method provides reasonable bandwidth results for bi/multimodal distributions [*Oliveira et al*., 2013]. Note that in cases with small sample size for complex models, which are mixtures of 3, 4, or 5 circular distributions, none of the smoothing parameter selectors will provide accurate results. To this end, we estimated an optimal bandwidth for each station from bootstrap resampling (which is the resampling with replacement). The annual maximum precipitation of the 60 extreme events from 1951 to 2010 was resampled 1000 times and each time a bandwidth was estimated from the new sample of 30 extremes using *LCV* method. The median value of the 1000 bandwidth estimates was taken as a representative optimal bandwidth for a particular station.

2.2. Results From Robust Approach

Before discussing seasonality results based on kernel circular density for our study locations, we first examined circular density estimates for the three cases of synthetic data discussed in section 1.3. Density estimates for synthetic data are presented in Figure 4. Note that bandwidth for each case was estimated using *LCV* method. Probability density estimates are assessed for significance based on resampling technique. Resampling techniques provide an idea of the nature of the uncertainty resulting from sampling errors and

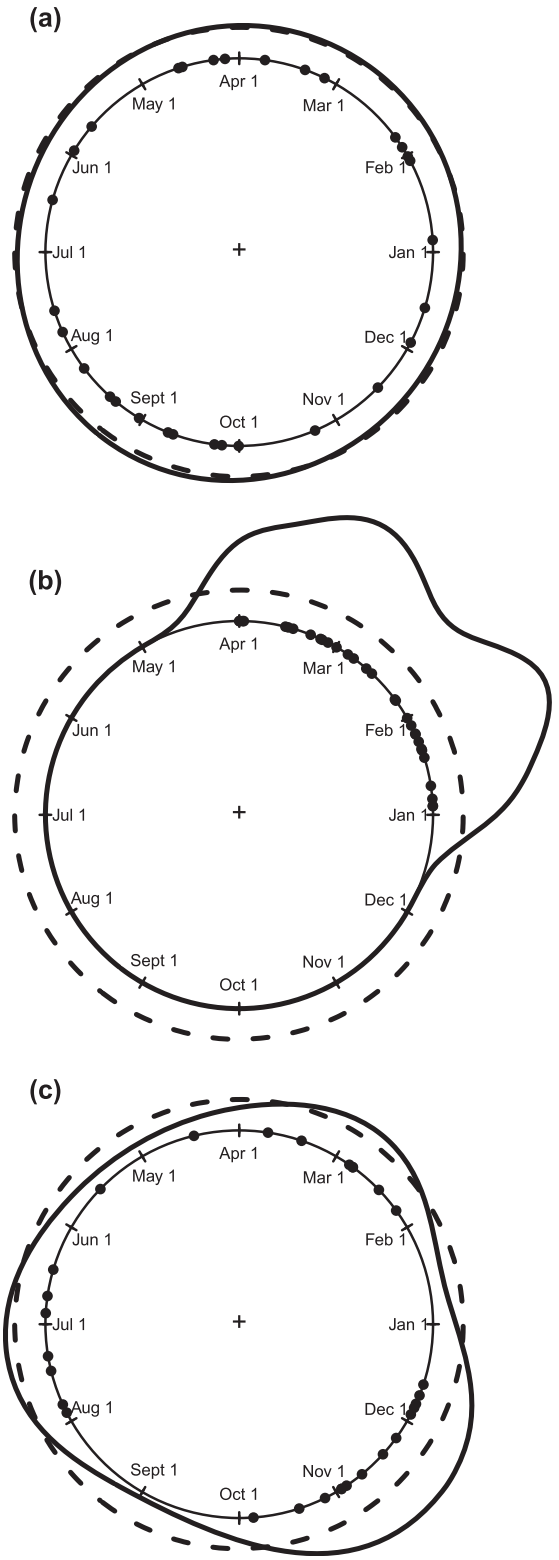

Figure 4. Nonparametric circular probability density estimates for three types of synthetic data. Probability density estimates are assessed for significance based on density estimates using resampled data. A median estimate is obtained from the ensemble of distributions resulting from bootstrap resampling ($N = 1000$).

internal variability [*Kharin and Zwiers*, 2005]. For our study, uncertainty was measured using a bootstrap method [*Rust et al.*, 2011]. In Figure 4, the dashed lines represent median estimate for significance based on density estimates using resampled data ($N = 1000$). Each of our resampled data comprise of a uniform distribution with no seasonality. We checked the significance of the type of distribution: uniform (no seasonality) versus nonuniform (seasonality) as done for the four uniformity tests. In other words, we assessed the significance based on point-by-point estimate of variability against the assumed uniform distribution (null). From Figure 4, we can see that estimates of kernel circular density successfully captures the actual distribution of data and seasonality therein, for all the three cases. For the data case (c), the estimates of circular density capture all three distinct modes as shown in Figure 4c. Although estimates of kernel density are sensitive to the smoothing parameter, this approach affords flexibility in capturing multiple modes in the seasonality and is superior to traditional methods based on measures to summarize circular random variables and the four nonparametric statistical tests. As noted previously, capturing multimodality in the seasonal distribution of the extreme precipitation dates is extremely important for a variety of hydrologic applications contexts, especially the timing of seasonality-specific decisions for infrastructure maintenance and assessment of regional hydrologic change. To this end, we used our approach to assess the seasonality of annual maximum daily precipitation for all 10 stations. Using the optimal bandwidth (discussed in section 2.1), kernel circular density was computed for each station based on the calendar dates of annual maximum daily precipitation for the period 1951–2010. The circular density estimates for Lewiston, Maine is presented in Figure 5. Note that in Figure 5, circular data are summarized using a Rose diagram. For Lewiston, Maine, although the circular distribution appears close to uniform, two seasonal modes are also visible, one from September to January and another from March to July. Distributions for 5 out of 10 stations exhibit similar seasonal pattern, while for the remaining 5 stations, kernel density estimates show somewhat unimodal seasonal pattern spanning the June–January period.

3. Temporal Changes in Seasonality

As noted previously, several studies have examined temporal changes in extreme rainfall magnitude

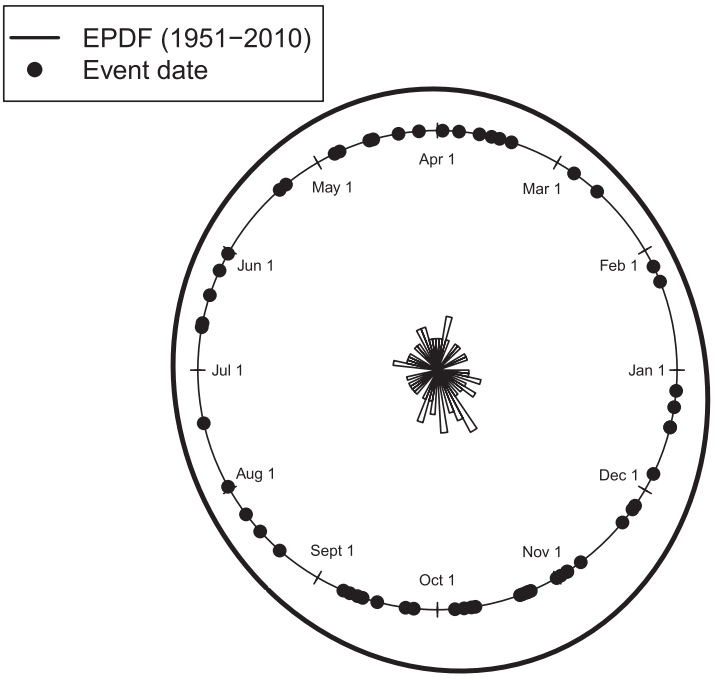

Figure 5. Empirical Probability Density Function (EPDF) estimates based on the calendar dates of annual maximum daily precipitation for Lewiston, Maine. Bandwidth for the kernel density estimates is evaluated using the likelihood cross-validation method.

and intensity, and found a general trend toward increases in the northeast United States. In this context, a salient question is that of examining the trends in the seasonality of extreme rainfall. In this section, we present an assessment of temporal changes in seasonality of daily extreme precipitation based on both the traditional circular statistical analysis method as well as the kernel circular density method. Change point analysis has been widely used to detect changes in time series statistics for linear data. We used change point analysis to detect the change in mean direction ($\overline{\theta}$) and the results are presented in Table S2. We can see that only Lewiston shows the significant change in $\overline{\theta}$ (the change point is at 21October). The limitation of this analysis for the circular data is that the underlying distribution is unimodal [*Ghosh et al.*, 1999] and it is not able to capture the change at multiple points.

In the past, numerous studies have used moving window analysis to assess the temporal changes in the precipitation extremes. For the circular approach, moving window analysis is useful for assessing the change in seasonality if the seasonal distribution is strongly unimodal and the variability does not show any sharp decrease with time. We present an example of such analysis for Presque Isle, Maine in Figure 6. A 30 year moving window estimates of $\overline{\theta}$ and ρ is shown in Figure 6. We can see that $\overline{\theta}$ and ρ do not exhibit any specific trend with time; the annual precipitation maxima typically occur during September. The seasonality in this case is strongly unimodal as represented by large value of ρ. For most of the stations, however, the seasonal pattern of extreme rainfall is diverse with small ρ and high *csd* as seen from our analysis in section 1.2. For such cases, the moving window analysis cannot completely capture the actual nature of seasonality. In addition, the appropriate estimation of bandwidth is difficult if we want to use the kernel density method with the moving window analysis. Herein, we selected two 30 year blocks (1951–1980 and 1981–2010) of annual maximum daily precipitation for assessing the temporal change in seasonality.

3.1. Results From Traditional Circular Approach

Here we present an assessment of temporal changes in seasonality based on traditional circular approach. Parameters $\overline{\theta}$ and ρ were estimated for each block of annual maximum precipitation separately for all the 10 stations and listed in Table 3. From Table 3, we can see that for three stations: Brassua Dam, Corinna, and Lewiston, the mean date of occurrence $\overline{\theta}$ has shifted from Fall season (respectively months of October, September, and November) toward earlier months (respectively, months of August, July, and July) for the recent time period. For all the three stations, the variability in the extreme precipitation dates has increased for the recent time period (shown by the decreasing value of ρ). Although for Eastport also there is shift in the mean date $\overline{\theta}$ toward earlier months; however there is decrease in variability for the recent time period. Farmington is the only one station where the mean date $\overline{\theta}$ has markedly shifted from earlier months toward later part of the year (March (Spring) to August (Fall)) for the recent time period. On the other hand, for Portland and Gardiner, the mean date of occurrence $\overline{\theta}$ is highly variable for both time periods indicating no seasonal pattern. Similarly, for other two stations: Presque Isle and Woodland, $\overline{\theta}$ and ρ indicate that there is unimodal seasonal pattern occurring during Fall season for both time periods. Again these results

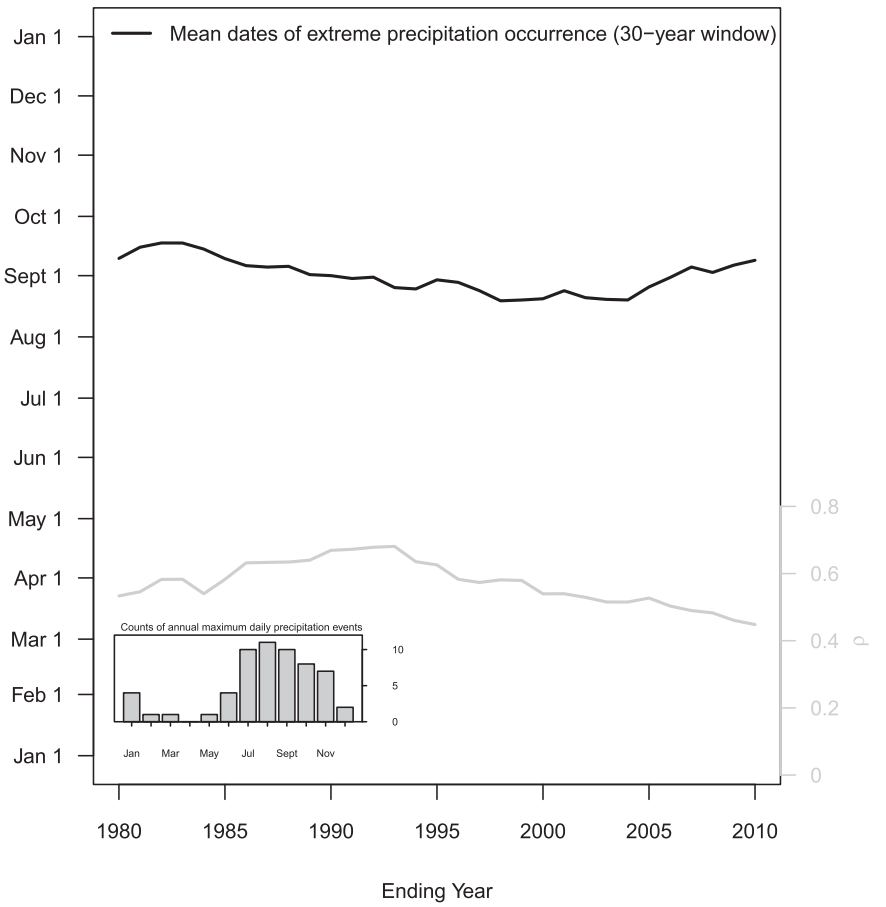

Figure 6. A 30 year moving window estimate of seasonality for Presque Isle, Maine shown by the mean date $\bar{\theta}$ and variability ρ for the period 1951–2010.

strengthen the fact that for most of stations, the seasonal pattern of extreme rainfall is diverse and complex for both time periods as we previously observed from the complete record (stationary) in section 1.2. Specifically three statistical measures provided us important information regarding the seasonality for both time periods and changes therein for stations with distinct unimodal seasonality pattern like Presque Isle and Woodland. However, for other stations where there is diversity in the seasonal pattern, these metrics were not able to completely decipher the seasonality change.

Table 3. Seasonality of Annual Maximum Daily Precipitation for the Periods 1951–1980 and 1981–2010, Estimated Separately From the Circular Statistical Analysis

	1951–1980						1981–2010					
	Circular Statistics		Uniformity Tests				Circular Statistics		Uniformity Tests			
Station	$\bar{\theta}$	ρ	Rayleigh	Rao Spacing	Kuiper	Hewitt Test	$\bar{\theta}$	ρ	Rayleigh	Rao Spacing	Kuiper	Hewitt Test
Brassua Dam	4.94 (12 Oct)	0.45	0.45**	150.14	2.03**	32	3.77 (5 Aug)	0.38	0.38**	150.65	1.73*	33**
Corinna	4.55 (20 Sep)	0.35	0.35**	151.40*	1.81**	31	3.46 (19 Jul)	0.23	0.23	124.84	1.28	31
Eastport	5.58 (18 Nov)	0.11	0.11	122.96	1.04	29	4.31 (6 Sep)	0.23	0.23	123.72	1.27	29
Farmington	1.08 (2 Mar)	0.16	0.16	111.50	1.09	27	3.85 (10 Aug)	0.19	0.19	111.87	1.23	30
Gardiner	5.55 (17 Nov)	0.24	0.24	155.82*	1.55	29	4.17 (29 Aug)	0.25	0.25	118.65	1.48	33**
Lewiston	5.52 (15 Nov)	0.36	0.36**	159.33**	2.00**	33*	3.44 (17 Jul)	0.17	0.17	117.57	1.29	27
Millinocket	4.85 (7 Oct)	0.25	0.25	118.50	1.40	27	4.35 (8 Sep)	0.39	0.39**	123.33	1.80**	31
Portland	6.23 (26 Dec)	0.20	0.20	137.74	1.50	31	5.15 (25 Oct)	0.27	0.27	159.86**	1.89**	33*
Presque Isle	4.35 (8 Sep)	0.53	0.53**	163.42**	2.37**	33*	4.33 (7 Sep)	0.45	0.45**	142.00	2.08**	31
Woodland	4.75 (1 Oct)	0.42	0.42**	132.81	1.71*	33**	5.14 (24 Oct)	0.31	0.31*	155.21*	1.65*	33**

**p value ≤ 0.05; *$0.05 < p$ value < 0.1.

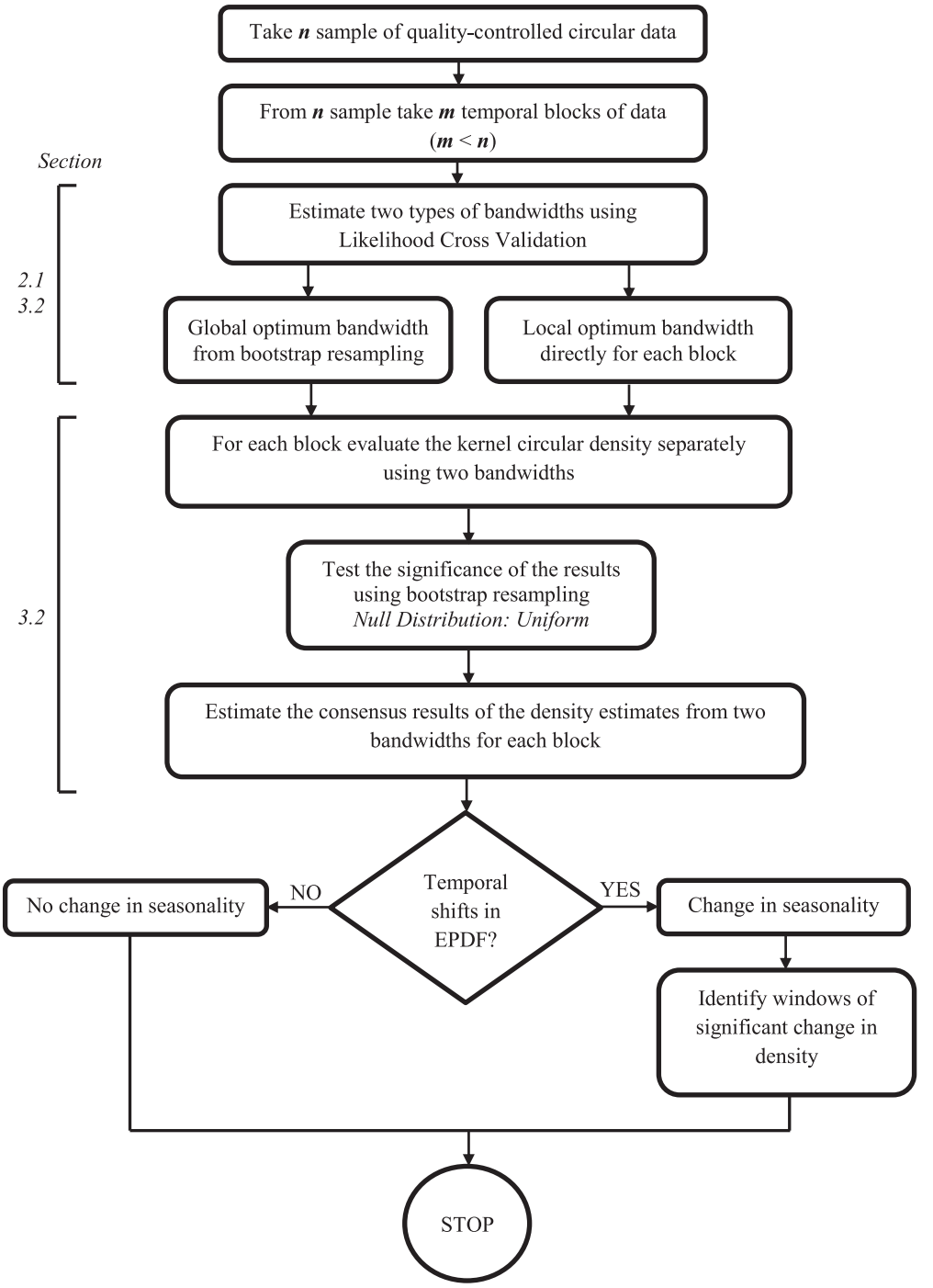

Figure 7. Schematic diagram showing the nonparametric framework for quantifying distribution of seasonality and temporal changes therein.

In addition to these exploratory data analysis, three nonparametric uniformity tests: Rayleigh, Rao Spacing, and Kuiper as well as nonparametric Hewitt test were performed to test the null hypothesis of no seasonal variation in extreme precipitation event dates for each block of annual maximum precipitation data separately, and the results are listed in Table 3. As seen in Table 3, Rayleigh test statistics are significant for five stations for the earlier time period and for four stations for the recent time period; only for the three cases

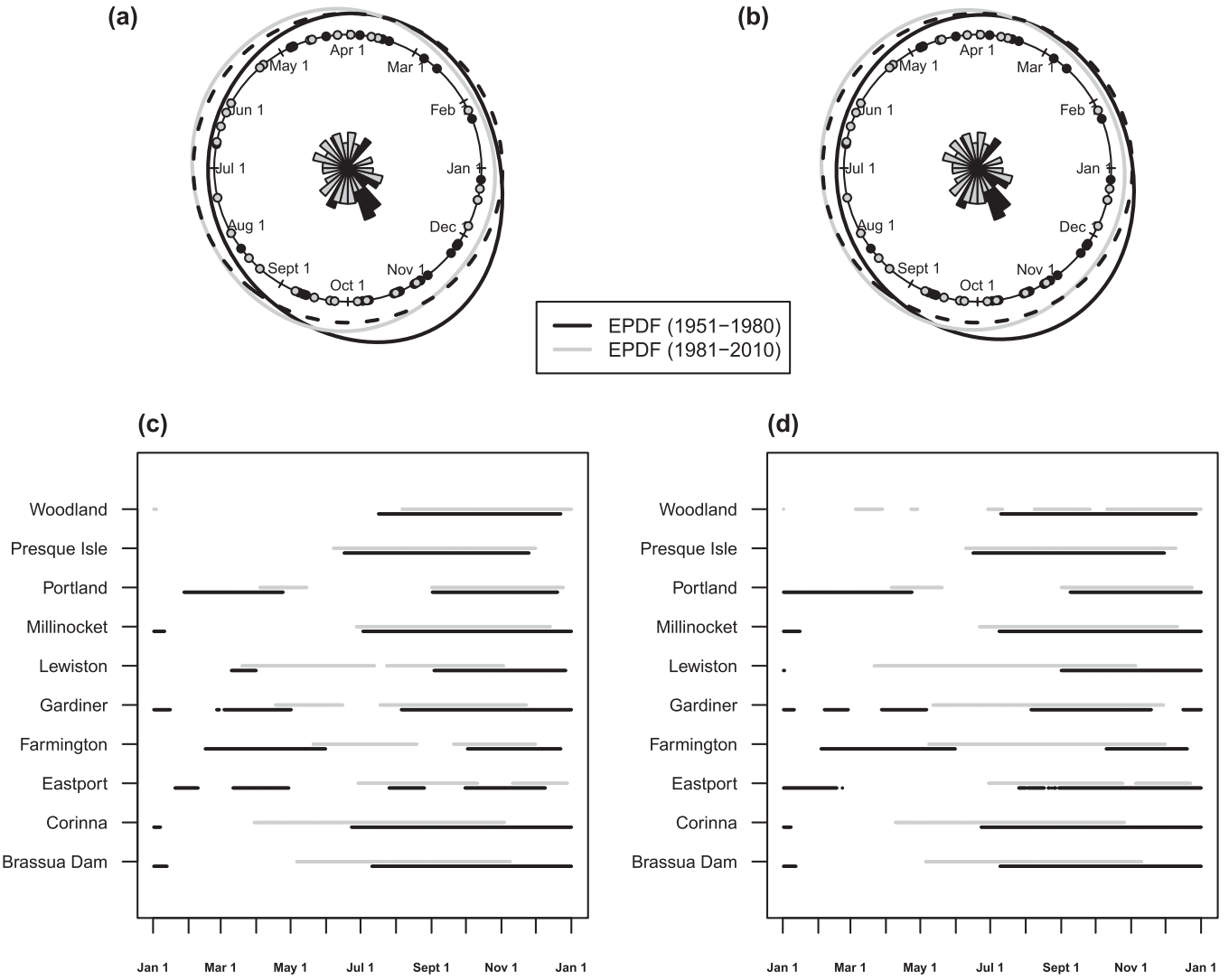

Figure 8. Probabilistic assessment of temporal changes in the seasonality of annual maximum daily precipitation. Two 30 year blocks (1951–1980 and 1981–2010) of annual maximum daily precipitation were considered for the analysis. Bandwidth for the kernel density is evaluated using *LCV* method. (a) Kernel circular density estimates for Lewiston, Maine for 1951–1980 (black) and 1981–2010 (grey) estimated using bandwidth optimized from complete data set (1951–2010; $n = 60$), (b) Kernel circular density estimates for Lewiston, Maine for 1951–1980 (black) and 1981–2010 (grey) estimated using two different bandwidths evaluated from two 30 year blocks of data separately; in Figures 8a and 8b, probability density estimates are assessed for significance based on density estimates using resampled data. A median estimate is obtained from the ensemble of distributions resulting from bootstrap resampling ($N = 1000$), (c) significant results estimated as described in Figure 8a for all stations, and (d) significant results estimated as described in Figure 8b for all stations.

are the test statistics significant for the same station for both time periods. Note that Rayleigh test is powerful (nonuniform) against unimodal alternatives only. Only for the three consensus stations, we can conclude that there is strong (unimodal) seasonality for both time periods. Rao Spacing test statistics are significant for four stations for the earlier time period and only for two stations for the recent time period; with no consensus stations for both time periods. Likewise, Kuiper test statistics are significant for five stations for both time periods; as for Rayleigh test, only for the three cases are the test statistics significant for the same station for both time periods. Note that both Rao Spacing and Kuiper tests are consistent (nonuniform) against unimodal as well as multimodal alternatives. For those stations where the test statistics are significant from either of these tests, we can conclude that there is existence of seasonality (uni or multimodal). Hewitt test statistics based on peak period of 3 months are significant for three stations for the earlier time period and for four stations for the recent time period; with only one consensus station. All of the tests results offer useful information regarding the nature of data and their seasonal distribution in the two time periods. However, for a number of cases, we did not obtain the consensus results from all these tests and the results

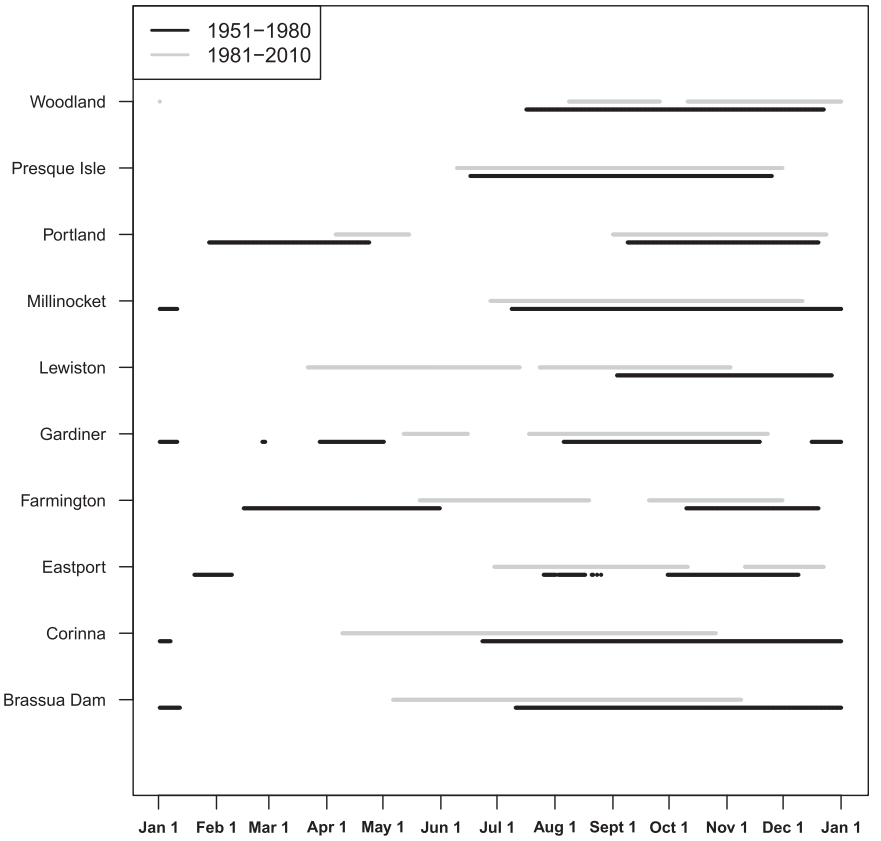

Figure 9. Temporal changes in seasonality for two 30 year blocks (1951–1980 and 1981–2010) of annual maximum daily precipitation estimated using two different bandwidth selection criteria (Figures 8c and 8d); black lines represent density estimates for the period 1951–1980, and grey lines represent the density estimates for the period 1981–2010. A "consensus" estimate is obtained based on the statistically significant overlapping time periods from the two (black and grey) estimates.

were inconclusive. For these cases, we expect our data to be complex and multimodal like the synthetic case (c). Subsequently, we used the robust approach based on the kernel circular density for assessing the temporal changes in seasonality of the extreme precipitation and presented in the next section.

3.2. Results From Robust Approach

A schematic diagram showing the steps to assess the temporal change in seasonality based on the nonparametric density approach is provided in Figure 7. As the results of kernel density, estimates are sensitive to bandwidth; here we used two different criteria to estimate bandwidth using *LCV* method. For the first criteria, a single optimized bandwidth is obtained for each station from the complete data set (1951–2010; $n = 60$) using the bootstrap resampling as described in section 2.1. For the second criteria, two different bandwidths were evaluated from two 30 year blocks of data separately for each station. Kernel circular density estimates were obtained for all stations for each time period separately. Density estimates for Lewiston, Maine obtained using bandwidth optimized from complete data set is shown in Figure 8a and using two different bandwidths evaluated from two 30 year blocks of data separately is shown in Figure 8b. Probability density estimates for the 1951–1980 (black) and 1981–2010 (grey) are assessed for significance based on density estimate using resampled data. A median estimate is obtained from the ensemble of distributions resulting from bootstrap resampling ($N = 1000$). From Figures 8a and 8b, we can see that the seasonal distribution of extreme precipitation events has changed from unimodal to somewhat uniform for the recent time periods, irrespective of the criteria used for the selection of bandwidth. Previously, significant mode is only concentrated in the October–January period; while for the recent period, the mode during this period has gotten weaker and there is simultaneous emergence of the significant mode during April–July period. Note that these results are sensitive to the threshold used to assess the significance.

Significant results of the density estimates using bandwidth optimized from complete data set are presented in Figure 8c for all 10 stations. From Figure 8c, we can see that for three stations (Woodland, Presque Isle, and Millinocket) there is no significant temporal change in seasonality with the distribution concentrated in the July-December period; while for other three stations (Brassua Dam, Corinna, and Lewiston), there is emergence of modes during Spring season for the recent time period. Moreover, for the remaining four stations, seasonal distribution is showing multimodal patterns for both time periods. Significant results of kernel circular density estimates using two different bandwidths evaluated from two 30 year blocks of data separately are presented in Figure 8d for all 10 stations. From Figure 8d, we can see that for Presque Isle there is no significant temporal change in seasonality with the distribution concentrated in the July-November period; while for four stations (Woodland, Brassua Dam, Corinna, and Lewiston), there is emergence of modes during Spring season for the recent time period. Moreover, for the remaining four stations, seasonal distribution is showing multimodal patterns for both time periods.

Above analysis corroborates the fact that the density estimates are influenced by the bandwidth selection criteria. To this end, we estimated the consensus results of the density estimates from Figures 8c and 8d. Consensus temporal changes in seasonality for two 30 year blocks (1951–1980 and 1981–2010) of annual maximum precipitation estimated using two different bandwidth selection criteria (Figures 8c and 8d) is presented in Figure 9; black lines represent density estimates for the period 1951–1980 and grey lines represent the density estimates for the period 1981–2010. A "consensus" estimate was obtained based on the statistically significant overlapping time periods from the two (black and grey) estimates. From Figure 9, we can see that for three stations (Woodland, Presque Isle, and Millinocket) there is no significant temporal change in seasonality with the distribution concentrated in the July-December period; while for other three stations (Brassua Dam, Corinna, and Lewiston), there is emergence of modes during Spring season for the recent time period. Moreover, for the remaining four stations, significant seasonal distribution is showing multimodal patterns for both time periods. Emergence of significant modes during Spring season has a significant impact on the repair and maintenance of the infrastructures. Heavy rainfall events that are now more likely to occur earlier in the year should shift decisions based on managing those events (e.g., clearing blocked or clogged culverts, regrooming roadside ditches, etc.) earlier in the year as well.

4. Summary and Conclusions

In this paper, we presented a circular statistical approach for the assessment of temporal changes in seasonality of extreme precipitation across the state of Maine. Two 30 year blocks (1951–1980 and 1981–2010) of annual maximum daily precipitation were used for analysis. Preliminary assessment of seasonality was done by evaluating mean date and variability of the date of occurrence of extreme precipitation events, the method previously used by four other studies [*Bayliss and Jones*, 1993; *Burn*, 1997; *Parajka et al*., 2009, 2010]. In addition, we also used four nonparametric tests: Rayleigh, Rao Spacing, Kuiper, and Hewitt test to check the null hypothesis of no seasonality against the alternative hypothesis of seasonality. These methods provided us some useful insight regarding the distribution of data and the seasonality therein; these methods worked perfectly well for the cases where the distribution of extreme event timing is unimodal (one dominant season) or uniform (no preferred season). However, distribution of extreme event timing tends to be more often multimodal. For such cases, results from one or all of these methods may be misleading. Daily precipitation records were used to develop records of calendar dates for extreme precipitation, and compute the circular probability distribution. Systematic exposition of methods used for seasonality assessment were presented in Figures 3 and 7.

Nonparametric circular density approach, used in this study, offers an adaptive alternative for an assessment of changes in seasonality over time. Note that the temporal changes in seasonality may appear due to weakening of modes within one season (Fall) and simultaneous strengthening of modes in one or all of the other seasons (Winter, Spring, or Summer) or it may appear due to the emergence of completely new modes (shifting of mode from Fall to Spring season). The kernel circular density approach accommodates the range of seasonality change types noted above. It is worth noting that estimates of the kernel circular density are sensitive to: (a) threshold used to assess the significance and (b) the bandwidth selection criteria. To address the latter issue, we used two different criteria to estimate two bandwidths using *LCV*

approach. Subsequently, temporal changes (based on two 30 year blocks) in seasonality were evaluated based on a consensus approach, as shown in Figure 9.

Temporal changes in seasonality of extreme precipitation events have salience for both hydroclimatic change studies and infrastructure adaptation considerations. These results pave the way for concurrent evaluation of possible future changes in seasonality based on gridded data obtained from different climate model simulations. Moreover, the shifting of extreme storm timing offers municipal officials an opportunity to revisit the timing of seasonality-specific decisions. For example, decisions linked to stormwater management (e.g., clearing blocked or clogged culverts, repairing roadside ditches) can be appropriately rescheduled to be in line with identified changes in the timing of heavy rainfall events.

In this study, no attempt was made to seek climatological explanations for observed changes in the seasonality of extreme precipitation. Efforts to understand the causal factors involve analyses of seasonal availability and delivery pathways of atmospheric moisture, which in turn are determined by the large-scale general circulation of the atmosphere [*Hirschboeck,* 1988; *Nakamura et al.*, 2013], as well as its moisture carrying capacity. Regional-scale analyses based on our approach have the potential to offer important insights regarding changing patterns of rainfall extremes. Our ongoing work seeks to generalize the proposed approach for application to regional and global scales.

Acknowledgments
This work is supported by National Science Foundation EPSCoR award EPS-0904155 to Maine EPSCoR at the University of Maine. The data used in this study are available at http://cdiac.ornl.gov/ftp/ushcn_daily/. The authors express their sincere gratitude to the three reviewers and Associate Editor for their thoughtful reviews and constructive feedback.

References

Agostinelli, C., and U. Lund (2013), R Package 'Circular': Circular Statistics (Version 0.4–7). [Available at https://r-forge.r-project.org/projects/circular/.]
Bayliss, A. C., and R. C. Jones (1993), *Peaks-Over-Threshold Flood Database: Summary Statistics and Seasonality, Report no. 121*, Inst. of Hydrol., Wallingford, U. K.
Burn, D. H. (1997), Catchment similarity for regional flood frequency analysis using seasonality measures, *J. Hydrol.*, *202*(1-4), 212–230.
Cheng, L., and A. AghaKouchak (2014), Nonstationary precipitation intensity-duration-frequency curves for infrastructure design in a changing climate, *Sci. Rep.*, *4*, 7093.
Cook, J. (1910), Centre of gravity of annual statistics, *Nature*, *83*, 125–126.
DeGaetano, A. T. (2009), Time-dependent changes in extreme-precipitation return-period amounts in the continental United States, *J. Appl. Meteorol. Climatol.*, *48*(10), 2086–2099.
Easterling, D. R., T. C. Peterson, and T. R. Karl (1996), On the development and use of homogenized climate datasets, *J. Clim.*, *9*(6), 1429–1434.
Fahidy, T. Z. (2013), On the Potential application of uniformity tests in circular statistics to chemical processes, *Int. J. Chem.*, *5*(1), 31–38.
Ghosh, K., S. R. Jammalamadaka, and M. Vasudaven (1999), Change-point problems for the von Mises distribution, *J. Appl. Stat.*, *26*(4), 423–434.
Groisman, P. Y., R. W. Knight, and T. R. Karl (2001), Heavy precipitation and high streamflow in the contiguous United States: Trends in the twentieth century, *Bull. Am. Meteorol. Soc.*, *82*(2), 219–246.
Hall, P., G. S. Watson, and J. Cabrera (1987), Kernel density estimation with spherical data, *Biometrika*, *74*(4), 751–762.
Hershfield, D. M. (1961), Rainfall frequency atlas of the united states for durations from 30 minutes to 24 hours and return periods from 1 to 100 years, *Weather Bur. Tech. Pap. 40*, U.S. Weather Bur., Washington, D. C. [Available at http://www.nws.noaa.gov/oh/hdsc/PF_documents/TechnicalPaper_No40.pdf.]
Hewitt, D., J. Milner, A. Csima, and A. Pakula (1971), On Edwards' criterion of seasonality and a non-parametric alternative, *Br. J. Prev. Soc. Medicine*, *25*(3), 174–176.
Higgins, R. W., and V. E. Kousky (2013), Changes in observed daily precipitation over the United States between 1950–79 and 1980–2009, *J. Hydrometeorol.*, *14*, 105–121.
Hirschboeck, K. K. (1988), Climate and floods, *Natl. Water Summary*, *89*, 67–88.
Jacobson, G. L., I. J. Fernandez, P. A. Mayewski, and C. V. Schmitt (Eds.) (2009), *Maine's Climate Future: An Initial Assessment*, Univ. of Maine, Orono. [Available at http://climatechange.umaine.edu/files/Maines_Climate_Future.pdf.]
Jain, S., and U. Lall (2000), Magnitude and timing of annual maximum floods: Trends and large-scale climatic associations for the Blacksmith Fork River, Utah, *Water Resour. Res.*, *36*(12), 3641–3651, doi:10.1029/2000WR900183.
Jain, S., and U. Lall (2001), Floods in a changing climate: Does the past represent the future?, *Water Resour. Res.*, *37*(12), 3193–3205, doi:10.1029/2001WR000495.
Jammalamadaka, S. R. (1972), Bahadur efficiencies of some tests for uniformity on the circle, *Ann. Math. Stat.*, 468–479.
Jammalamadaka, S. R., and A. SenGupta (2001), *Topics in Circular Statistics*, vol. 5, World Sci., Singapore.
Karl, T. R., and R. W. Knight (1998), Secular trend of precipitation amount, frequency, intensity in the United States, *Bull. Am. Meteorol. Soc.*, *79*, 231–242.
Khaliq, M. N., T. B. M. J. Ouarda, J. C. Ondo, P. Gachon, and B. Bobée (2006), Frequency analysis of a sequence of dependent and/or non-stationary hydro-meteorological observations: A review, *J. Hydrol.*, *329*(3), 534–552.
Kharin, V. V., and F. W. Zwiers (2005), Estimating extremes in transient climate change simulations, *J. Clim.*, *18*(8), 1156–1173.
Lall, U. (1995), Recent advances in nonparametric function estimation: Hydrologic applications, *Rev. Geophys.*, *33*(S2), 1093–1102.
Lee, A. (2010), Circular data, *WIREs Comput. Stat.*, *2*(4), 477–486.
Lee, J. J., H. H. Kwon, and T. W. Kim (2012), Spatio-temporal analysis of extreme precipitation regimes across South Korea and its application to regionalization, *J. Hydroenviron. Res.*, *6*(2), 101–110.
Mardia, K. V., and P. E. Jupp (2000), *Directional Statistics*, John Wiley, N. Y.
Markham, C. G. (1970), Seasonality of precipitation in the United States, *Ann. Assoc. Am. Geogr.*, *60*(3), 593–597.

Milly, P. C. D., J. Betancourt, M. Falkenmark, R. M. Hirsch, Z. W. Kundzewicz, D. P. Lettenmaier, and R. J. Stouffer (2008), Stationarity is dead: Whither water management?, *Science*, *319*, 573–574.
Mirhosseini, G., P. Srivastava, and L. Stefanova (2013), The impact of climate change on rainfall Intensity–Duration–Frequency (IDF) curves in Alabama, *Reg. Environ. Change*, *13*(1), 25–33.
Moberg, A., et al. (2006), Indices for daily temperature and precipitation extremes in Europe analyzed for the period 1901–2000, *J. Geophys. Res.*, *111*, D22106, doi:10.1029/2006JD007103.
Montanari, A., and D. Koutsoyiannis (2014), Modeling and mitigating natural hazards: Stationarity is immortal!, *Water Resour. Res.*, *50*, 9748–9756, doi:10.1002/2014WR016092.
Nakamura, J., U. Lall, Y. Kushnir, A. W. Robertson, and R. Seager (2013), Dynamical structure of extreme floods in the U.S. Midwest and the United Kingdom, *J. Hydrometeorol.*, *14*, 485–504.
Oliveira, M., R. M. Crujeiras, and A. Rodríguez-Casal (2012), A plug-in rule for bandwidth selection in circular density estimation, *Comput. Stat. Data Anal.*, *56*(12), 3898–3908.
Oliveira, M., R. M. Crujeiras, and A. Rodríguez-Casal (2013), Nonparametric circular methods for exploring environmental data, *Environ. Ecol. Stat.*, *20*(1), 1–17.
Pal, I., B. T. Anderson, G. D. Salvucci, and D. J. Gianotti (2013), Shifting seasonality and increasing frequency of precipitation in wet and dry seasons across the US, *Geophys. Res. Lett.*, *40*, 4030–4035, doi:10.1002/grl.50760.
Parajka, J., S. Kohnová, R. Merz, J. Szolgay, K. Hlavčová, and G. Blöschl (2009), Comparative analysis of the seasonality of hydrological characteristics in Slovakia and Austria, *Hydrol. Sci. J.*, *54*(3), 456–473.
Parajka, J., et al. (2010), Seasonal characteristics of flood regimes across the Alpine–Carpathian range, *J. Hydrol.*, *394*(1), 78–89.
Pryor, S. C., and J. T. Schoof (2008), Changes in the seasonality of precipitation over the contiguous USA, *J. Geophys. Res.*, *113*, D21108, doi: 10.1029/2008JD010251.
Rajagopalan, B., and U. Lall (1995), Seasonality of precipitation along a meridian in the western United States, *Geophys. Res. Lett.*, *22*(9), 1081–1084.
Rogerson, P. A. (1996), A generalization of Hewitt's test for seasonality, *Int. J. Epidemiol.*, *25*(3), 644–648.
Rust, H. W., M. Kallache, H. J. Schellnhuber, and J. Kropp (2011), *Confidence Intervals for Flood Return Level Estimates Using a Bootstrap Approach*, edited by J. Kropp and H. J. Schellnhuber, pp. 61–81, Springer, Heidelberg, Germany.
Salas, J. D., and J. Obeysekera (2013), Revisiting the concepts of return period and risk for nonstationary hydrologic extreme events, *J. Hydrol. Eng.*, *19*(3), 554–568.
Sen Gupta, A., S. Jain, and J.-S. Kim (2011), Past climate, future perspective: An exploratory analysis using climate proxies and drought risk assessment to inform water resources management and policy in Maine, USA, *J. Environ. Manage.*, *92*(3), 941–947.
Taylor, C. C. (2008), Automatic bandwidth selection for circular density estimation, *Comput. Stat. Data Anal.*, *52*, 3493–3500.
Walsh, R. P. D., and D. M. Lawler (1981), Rainfall seasonality: Description, spatial patterns and change through time, *Weather*, *36*(7), 201–208.
Zolina, O., C. Simmer, A. Kapala, S. Bachner, S. Gulev, and H. Maechel (2008), Seasonally dependent changes of precipitation extremes over Germany since 1950 from a very dense observational network, *J. Geophys. Res.*, *113*, D06110, doi:10.1029/2007JD008393.